AGU ADVANCING EARTH AND SPACE SCIENCE

Geophysical Research Letters®

RESEARCH LETTER
10.1029/2021GL095922

Tropical Cyclone Outer Size Impacts the Number and Location of Tornadoes

Marco Paredes[1], Benjamin A. Schenkel[2,3], Roger Edwards[4], and Michael Coniglio[3,5]

[1]Department of Earth and Environment, Florida International University, Miami, FL, [2]Cooperative Institute for Severe and High-Impact Weather Research and Operations, University of Oklahoma, Norman, OK, [3]NOAA National Severe Storms Laboratory, Norman, OK, [4]NOAA/NWS Storm Prediction Center, Norman, OK, [5]School of Meteorology, University of Oklahoma, Norman, OK

Key Points:

- Tornadoes occur farther from and over a broader region relative to the center of larger tropical cyclones (TCs)
- Larger TCs more frequently spawn enhanced numbers of tornadoes per 6-h period
- Larger TCs are associated with broader regions of favorable convective-scale kinematic environments for tornadoes

Supporting Information:

Supporting Information may be found in the online version of this article.

Correspondence to:

B. A. Schenkel,
benschenkel@gmail.com

Citation:

Paredes, M., Schenkel, B. A., Edwards, R., & Coniglio, M. (2021). Tropical cyclone outer size impacts the number and location of tornadoes. *Geophysical Research Letters*, *48*, e2021GL095922. https://doi.org/10.1029/2021GL095922

Received 31 AUG 2021
Accepted 20 NOV 2021

Author Contributions:

Conceptualization: Marco Paredes
Data curation: Benjamin A. Schenkel
Formal analysis: Marco Paredes, Benjamin A. Schenkel, Roger Edwards, Michael Coniglio
Funding acquisition: Benjamin A. Schenkel, Roger Edwards, Michael Coniglio
Investigation: Marco Paredes, Benjamin A. Schenkel, Roger Edwards, Michael Coniglio
Methodology: Marco Paredes, Benjamin A. Schenkel, Roger Edwards, Michael Coniglio
Project Administration: Benjamin A. Schenkel
Resources: Benjamin A. Schenkel
Software: Marco Paredes, Benjamin A. Schenkel
Supervision: Benjamin A. Schenkel
Validation: Marco Paredes, Benjamin A. Schenkel
Visualization: Marco Paredes, Benjamin A. Schenkel

Abstract There remains no consensus on whether the outer size of the tropical cyclone (TC) wind field impacts tornado occurrence. This study statistically examines the relationship between TC outer size with both the number and location of tornadoes using multidecadal tornado reports, a reanalysis-derived TC outer size metric, and radiosonde data. These results show that larger TC spawn tornadoes that are located farther from and over a broader region relative to the cyclone center, although these changes do not entirely scale with TC outer size. Larger TCs are also associated with more frequent occurrence of tornadoes per 6 h, especially enhanced numbers of tornadoes. These changes in tornado occurrence in larger TCs may be due to a broadening of favorable helicity for tornadoes in the downshear sector, which may be partially offset by CAPE reductions in the left-of-shear quadrants.

Plain Language Summary Tropical cyclones (TCs) (also known as tropical depressions, storms, and hurricanes) with similar landfall locations and maximum wind speeds often spawn different numbers of tornadoes. One understudied factor that may explain these differences in tornado occurrence is how far the TC winds extend from its center, referred to as its outer size. This study investigates whether the outer size of the TC wind field impacts the number and location of tornadoes using tornado and TC observations, historical weather forecast data, and observations from balloon-borne weather instruments. These results show that larger TCs more frequently spawn tornadoes, which are associated with a broader region of tornado occurrence. Moreover, tornadoes tend to be located farther from the TC in storms with larger wind fields. These results are attributed to a broader set of radii with favorable vertical variations in wind speed and direction for tornadoes in larger TCs. These changes may be partially offset by reductions in temperature and moisture that may explain why the changes in tornado frequency and location are not more extreme in larger TCs. Together, these results suggest that the outer size of the TC is a key factor in forecasting tornadoes.

1. Introduction

Landfalling tropical cyclones (TCs) often produce tornadoes in addition to other hazards. Most tornadoes occur during the afternoon within 100–500 km of the TC center during the 48-h period before and after landfall (Novlan & Gray, 1974; Schultz & Cecil, 2009). Compared to their non-TC counterparts, TC tornadoes typically: 1) are less damaging (Edwards, 2010; Edwards, 2012), 2) are produced by "miniature" supercells (Spratt et al., 1997; Edwards et al., 2012), and 3) occur in strong vertical wind shear and sufficient thermodynamic instability concentrated over a shallow lower-tropospheric layer (McCaul, 1991; McCaul & Weisman, 1996). These favorable kinematic conditions are due to the TC warm-core structure and surface friction (Novlan & Gray, 1974; Gentry, 1983), while favorable thermodynamic environments are associated with weak convective inhibition and CAPE typical of the tropics (McCaul, 1991; Molinari et al., 2012). Moreover, recent work has shown that ambient deep-tropospheric vertical wind shear (VWS; i.e., the difference between the 850-and 200-hPa ambient winds) is a key factor controlling the number and TC-relative azimuthal location of tornadoes (Schenkel et al., 2020; Schenkel et al., 2021). However, we lack a complete understanding of the factors controlling the number and TC-relative radial location of tornadoes. One understudied factor that may impact the number and TC-relative radius of tornadoes is the outer size of the TC (McCaul, 1991). Indeed, TC outer size is crucial in describing the scale and magnitude of hazards (Lin et al., 2014; Chavas et al., 2017), and is the focus of this study.

Writing – original draft: Marco Paredes, Benjamin A. Schenkel, Roger Edwards, Michael Coniglio
Writing – review & editing: Marco Paredes, Benjamin A. Schenkel, Roger Edwards, Michael Coniglio

As previously alluded to, VWS strongly confines tornadoes to the downshear half of the TC (i.e., in the direction of the VWS vector) as VWS increases (Schenkel et al., 2020; Schenkel et al., 2021). In strongly sheared TCs, inner-core tornadoes (i.e., ≤200 km from TC center) are located in the downshear left quadrant (i.e., left and in the same direction as VWS vector), whereas outer region tornadoes occur downshear right (Schenkel et al., 2020; Schenkel et al., 2021). These VWS-induced patterns in tornado occurrence are due to two factors. First, VWS vertically tilts the TC downshear yielding an acceleration of the TC transverse circulation in a failed attempt to adiabatically restore thermal wind balance (Jones, 1995; Frank & Ritchie, 1999). This downshear strengthening of the TC overturning circulation is associated with enhanced ascent, moisture, and vertical wind shear (Molinari & Vollaro, 2008; Schenkel et al., 2020). Second, a constructive superposition between the TC and ambient winds, yields a nonlinear enhancement of helicity in the downshear sector, particularly downshear right (Gu et al., 2018; Schenkel et al., 2020).

Whereas VWS influences the TC-relative azimuth of tornadoes, this study hypothesizes that TC outer size controls the TC-relative radius and number of tornadoes. Indeed, idealized modeling has suggested that the outer rain bands, where most tornadoes occur, extend farther from TCs with broader wind fields (Stovern & Ritchie, 2016; Martinez et al., 2020). TC outer size is typically defined at radii with weak winds and sparse deep convection approximately characterized by radiative-subsidence balance (Emanuel, 2004; Chavas et al., 2015). Unlike TC intensity, many metrics have been used to define outer size (Merrill, 1984; Chan & Chan, 2013). However, most metrics have similar characteristics, including: 1) a lognormal distribution with a long right tail (Merrill, 1984; Chavas & Emanuel, 2010) and 2) slower changes in TC outer size than intensity yielding weak correlations between the two ($R \approx 0.3$; Merrill, 1984; Weatherford & Gray, 1988). TCs often grow throughout most of their life cycle before either contracting during cyclolysis or remaining unchanged during extratropical transition (Schenkel et al., 2018; Chen & Chavas, 2020).

Prior research has yet to conclude whether TC outer size impacts tornadoes. Early work has shown that many tornadoes occur inwards of the subjectively chosen 1005-hPa isopleth (Hill et al., 1966). Moreover, TCs producing >8 tornadoes during their lifetime were larger than storms that produced ≤1 tornado as shown using the radius of the outermost closed isobar (McCaul, 1991). This was hypothesized to be due to broader regions of favorable kinematic environments in larger TCs. However, this study did not consider if the increased number of tornadoes in large TCs was due to enhanced numbers of tornadoes per unit time or area or longer TC lifetimes given the greater resilience of large cyclones to unfavorable environments (Jones, 1995; Carrasco et al., 2014). More recent work found no relationship between the radius of the outermost closed isobar and number of tornadoes (Rhodes & Senkbeil, 2014). These inconsistent results may be due to considerable uncertainty in the radius of the outermost closed isobar from: 1) its subjective derivation that is method dependent and 2) its strong sensitivity to the environmental pressure field rather than being solely dependent on TC structure (Knaff et al., 2014). Moreover, these inconsistencies raise questions about whether TC outer size impacts tornadoes.

Given previous uncertainties, a study is necessitated to investigate the relationship between TC outer size and tornadoes using a long-term, objective metric. Hence, this study analyzes the influence of TC outer size on: 1) the number and location of tornadoes and 2) the favorability of convective-scale environments for tornadoes. We hypothesize that larger TCs produce more tornadoes located farther from the storm center and over a broader region due to a greater area with favorable kinematic environments. Our study uses multidecadal reanalysis-derived TC outer size and radiosonde data together with observed tornado reports. Specifically, our study will be the first to focus on the relationship between TC outer size and tornadoes including the following questions:

1. Do tornadoes occur farther from the center of and over a broader range of radii in larger TCs?
2. Are larger TCs associated with greater numbers of tornadoes per unit time and area?
3. Do larger TCs have a broader range of radii with favorable convective-scale environments for tornadoes?

2. Data and Methods

2.1. TC Tornado

Tornado starting location and time are obtained from the 25-yr (1995–2019) Storm Prediction Center TC tornado archive (Edwards, 2010). This data set collocates United States tornado reports with 6-h North Atlantic Best-Track TC track data from the National Hurricane Center (NHC; Landsea & Franklin, 2013). Each tornado

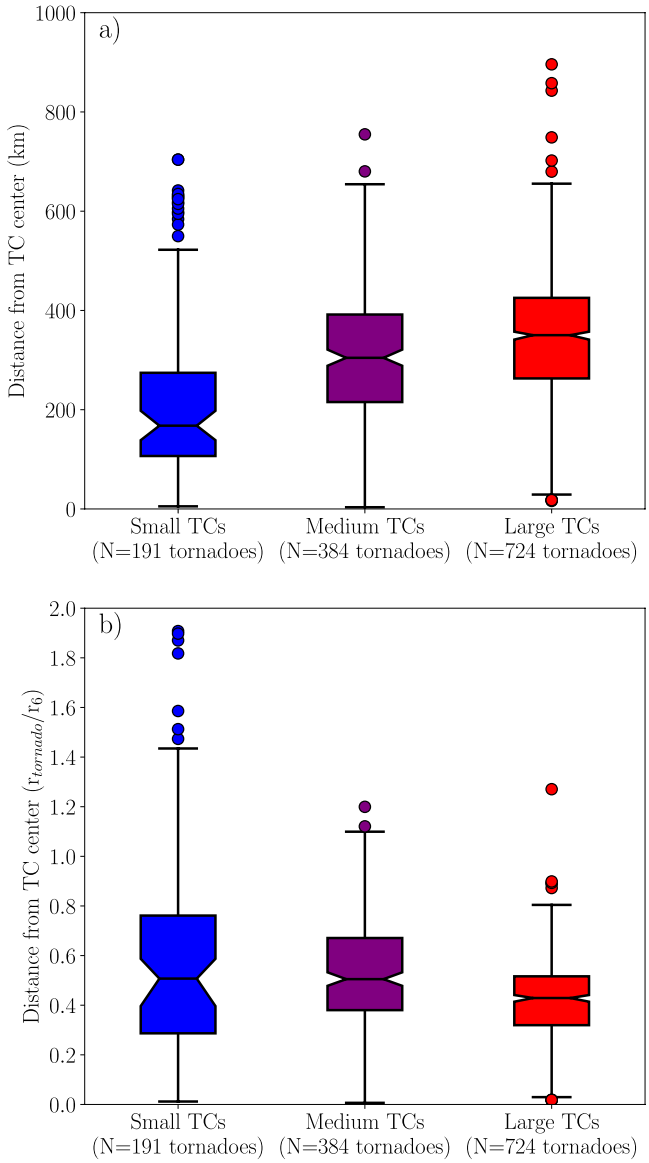

Figure 1. Box-and-whiskers plot of tornado distance in a (a) non-normalized (km) and (b) normalized ($r_{tornado}/r_6$) radial coordinate from the center of small, medium, and large tropical cyclones (TCs). The box plot displays the median (black horizontal line near box center) and its 95% confidence interval (box notches), interquartile range (box perimeter), whiskers (capped lines; [first datum above $[q_1-1.5(q_3-q_1)]$, first datum below $[q_3+1.5(q_3-q_1)]$]), and outliers (filled circles).

has been subjectively analyzed from observations using modern verification practices to confirm its association with a TC (Edwards, 2010). Our analysis examines TCs at tropical depression strength or greater, yielding a total of 1304 tornadoes in 90 TCs. However, TC tornadoes are undersampled for several reasons discussed extensively in prior work (e.g., inability to verify oceanic reports), which should be considered when interpreting our study (Edwards et al., 2012; Edwards, 2012). This study focuses on tornadoes per 6-h increment centered within ±3 h of each synoptic time rather than over the TC lifetime due to the short timescale variations in storm structure and its environment (Rios-Berrios & Torn, 2017; Schenkel et al., 2020). The TC outer size data used for each period are valid at each synoptic time. Our study examines those 6-h times in which the TC downshear half, where 92% of tornadoes occur (Schenkel et al., 2020), overlaps with the continental United States during ±3 hours of the verification time.

2.2. TC Outer Size

Our TC outer size metric is the radius at which the azimuthal-mean 925-hPa azimuthal wind equals 6 m s^{-1} (r_6). This metric has been used in prior TC tornado studies of convective-scale environments (Schenkel et al., 2021). We choose 925 hPa because it is typically the isobaric level with the strongest winds (Franklin et al., 2003; Alford et al., 2020). Operational wind field metrics are not used here since they are: 1) defined at a 10-m height resulting in artificial decreases as TCs move inland due to friction that can differ with the above surface winds (Hlywiak & Nolan, 2021; Chen & Chavas, 2020) and 2) may not encircle the TC radii where most tornadoes occur (Kimball & Mulekar, 2004; Demuth et al., 2006). TC outer size is computed from the 6-h 0.25° × 0.25° ECMWF fifth-generation (ERA5) reanalysis (Hersbach et al., 2020). Prior work has shown that TC track and outer size are well represented in the ERA5, especially in observation-dense regions (Bian et al., 2021; Schenkel et al., 2017).

To compute r_6, we first employ a vortex recentering algorithm given the uncertainties in both reanalysis and Best-Track data (Schenkel & Hart, 2012; Torn & Snyder, 2012). For each 6-h Best-Track TC location, the reanalysis position is identified as the mean location of the center of mass calculated from mean sea-level pressure, 850-hPa and 700-hPa geopotential height, and 925-hPa, 850-hPa, 700-hPa relative vorticity (Brammer, 2017). Using this location, we solve a Poisson equation with homogeneous boundary conditions within 500 km of the TC center to partition the ambient 925-hPa winds from the TC winds (Davis et al., 2008). We then exclude all data below the surface at 925 hPa and compute the ambient winds averaged within a 500-km radius of the TC (Galarneau & Davis, 2013; Schenkel et al., 2021). Finally, we compute r_6 by subtracting the ambient flow from the 925-hPa total winds, calculate its azimuthal-mean excluding data below the surface, and locate the radius at which the wind equals 6 m s^{-1} (Chavas & Vigh, 2014; Schenkel et al., 2017). We define small, medium, and large TCs as the lowest (<461 km), middle (461–668 km), and upper terciles (>668 km), respectively, from the r_6 distribution for all Atlantic storms from 1995–2019 (Carrasco et al., 2014).

2.3. VWS

A portion of our analysis uses a VWS-relative coordinate given its importance in determining the TC-relative azimuthal location of tornadoes (Schenkel et al., 2020; Schenkel et al., 2021). VWS data are calculated using 850-

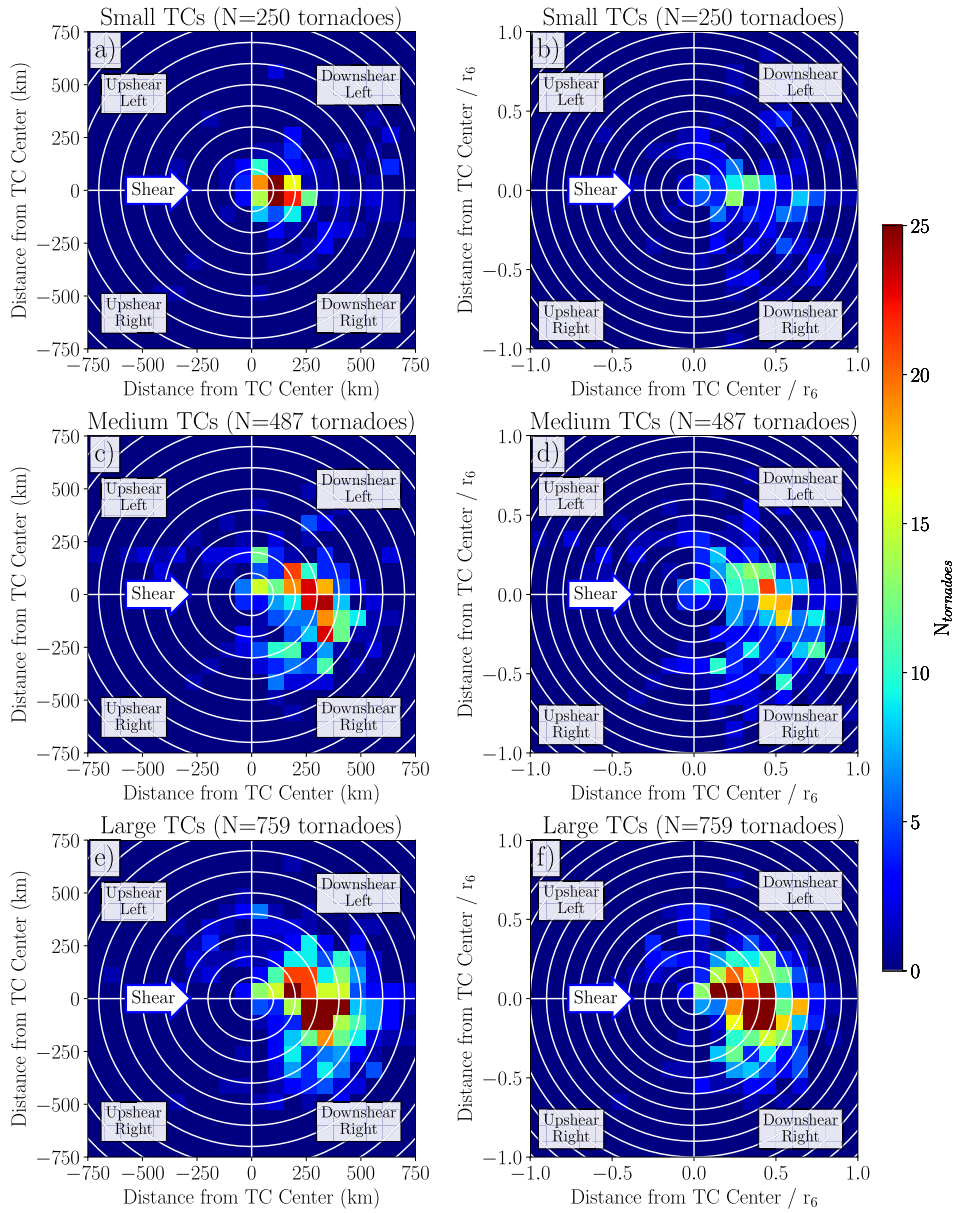

Figure 2. Plan view plot of tornado location ($N_{tornadoes}$) in a tropical cyclone (TC)-relative and VWS-relative coordinate for (a), (b) small, (c), (d) medium, and (e), (f) large TCs. A radial coordinate normalized by r_6 ($r_{tornado}/r_6$) at the time of tornado occurrence is used in (b), (d), and (f). Tornado reports and the VWS vector have been rotated such that the VWS vector (white arrow) is pointing to the right. Range rings are provided every 100 km for (a), (c), and (e), and every $0.1r_6$ for (b), (d), and (f).

and 200-hPa reanalysis winds by partitioning the ambient winds from the total wind field following the methods above (Davis et al., 2008). We then compute the average ambient winds within a 500-km radius of the TC center and calculate the difference between 850-hPa and 200-hPa winds (Rios-Berrios & Torn, 2017).

2.4. Radiosondes

To examine convective-scale TC environments, we examine radiosondes within 1.2 times r_6 for each North Atlantic TC from 1995–2019 in the NOAA Integrated Global Radiosonde Archive (IGRA), version 2 (Durre et al., 2006). In addition to the IGRA quality control algorithm (Durre et al., 2006), we employ the following

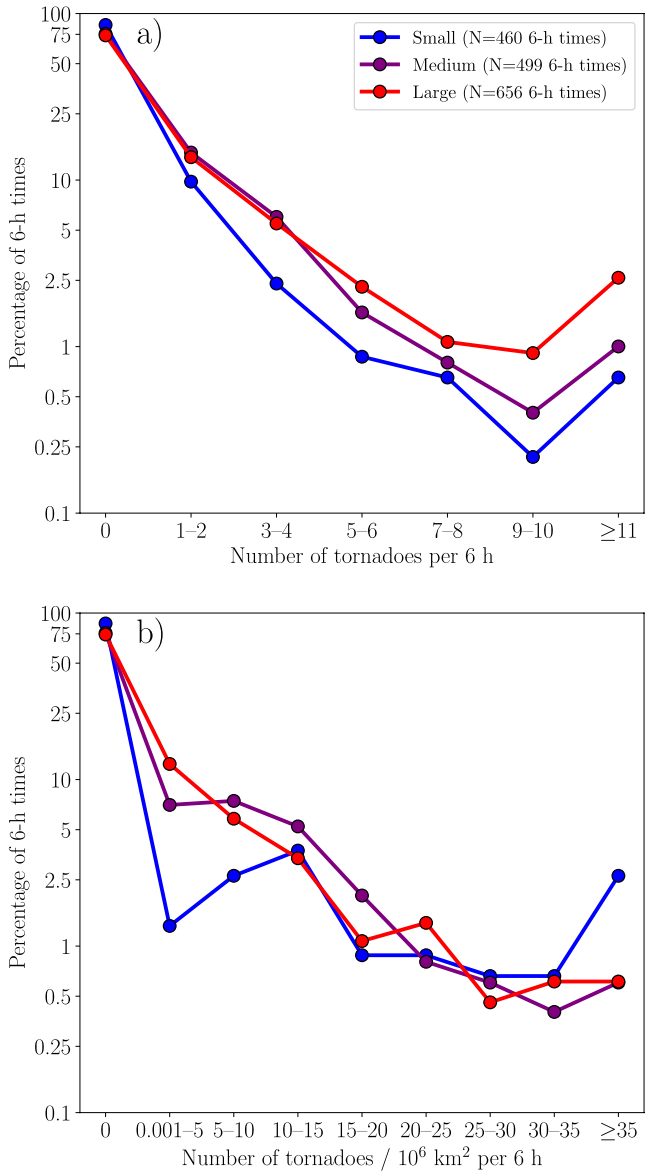

Figure 3. Histogram of (a) tornadoes per 6-h increment and (b) tornadoes / km^2 of the continental United States per 6-h increment for small, medium, and large tropical cyclones (TCs). Values are shown as a percentage relative to the total number of samples in each TC outer size subset.

vertical criteria (Molinari & Vollaro, 2008; Schenkel et al., 2020): 1) data present within 200 m of the surface and 2) data gaps must be ≤ 1 km. We exclude sondes within 75 km of the TC center given their large azimuthal advection by the TC (Molinari & Vollaro, 2008; Molinari & Vollaro, 2010) yielding 8586 radiosondes in 233 TCs (Figure S1).

These radiosondes diagnose the favorability of convective-scale environments for TC tornadoes and are not typically tornado proximity soundings (McCaul, 1991; Schenkel et al., 2020). Our analysis examines lower-tropospheric severe convective weather metrics typically used to diagnose favorable conditions associated with TC supercells (McCaul, 1991; McCaul & Weisman, 1996) including: 1) 0–3-km convective cell-relative helicity incorporating the cell-motion algorithm of Bunkers et al. (2014) and 2) 0–3-km CAPE using a 200-m mixed layer (Schenkel et al., 2020). Our analysis uses 1,000-sample bootstrap resampling with replacement for a two-tailed test at the 5% level to quantify statistical differences.

3. Results

3.1. Tornado Location

As outer size increases, tornadoes occur farther from and over a broader radii range from the TC center that does not wholly scale with outer size (Figure 1). Specifically, significant differences are shown among median radii of tornado occurrence for small (168 km), medium (305 km), and large (350 km) TCs. However, these values show no significant differences among categories when normalized by TC outer size with medians ranging between 0.4–0.5r$_6$. The range of tornado occurrence also shifts toward outer radii in larger TCs shown by comparing the range of whiskers between large (626 km) and small TCs (517 km; Hill et al., 1966). Nevertheless, these differences among categories are smaller relative to outer size changes, as shown by a reduction and inward shift in the whiskers of the normalized radius of tornado location.

Next, a VWS-relative and TC-relative coordinate is used (Figure 2) to examine the joint radial and azimuthal location of tornadoes with outer size. The left panels use a radial coordinate in km, whereas the TC-relative radius of each tornado has been normalized by r$_6$ in the right panels. Most tornadoes in small TCs are concentrated downshear within 300 km of the center in the non-normalized coordinate. As outer size increases, tornado distance from the TC center increases, yet there are no statistical changes in the VWS-relative azimuth of tornado location. Regardless of the outer size category, tornadoes near the TC center are downshear left and gradually shift with greater radius to the downshear right quadrant (Schenkel et al., 2020). Nonetheless, tornadoes occur over a greater azimuthal distance range as they shift toward broader radii in large TCs (547 km) compared to small TCs (329 km) according to the 90th percentile. The right panels show that median tornado distance from the center scales with outer size in both downshear quadrants, while the range of tornado occurrence decreases. Together, these results suggest an outward shift and broader area over which tornadoes in larger TCs occur that does not completely scale with outer size.

3.2. Tornado Number

The largest TCs are more frequently associated with enhanced numbers of tornadoes, likely due to a broader region of tornado occurrence (Figure 3). Specifically large TCs most frequently spawn ≥1 tornadoes per 6 h (23%

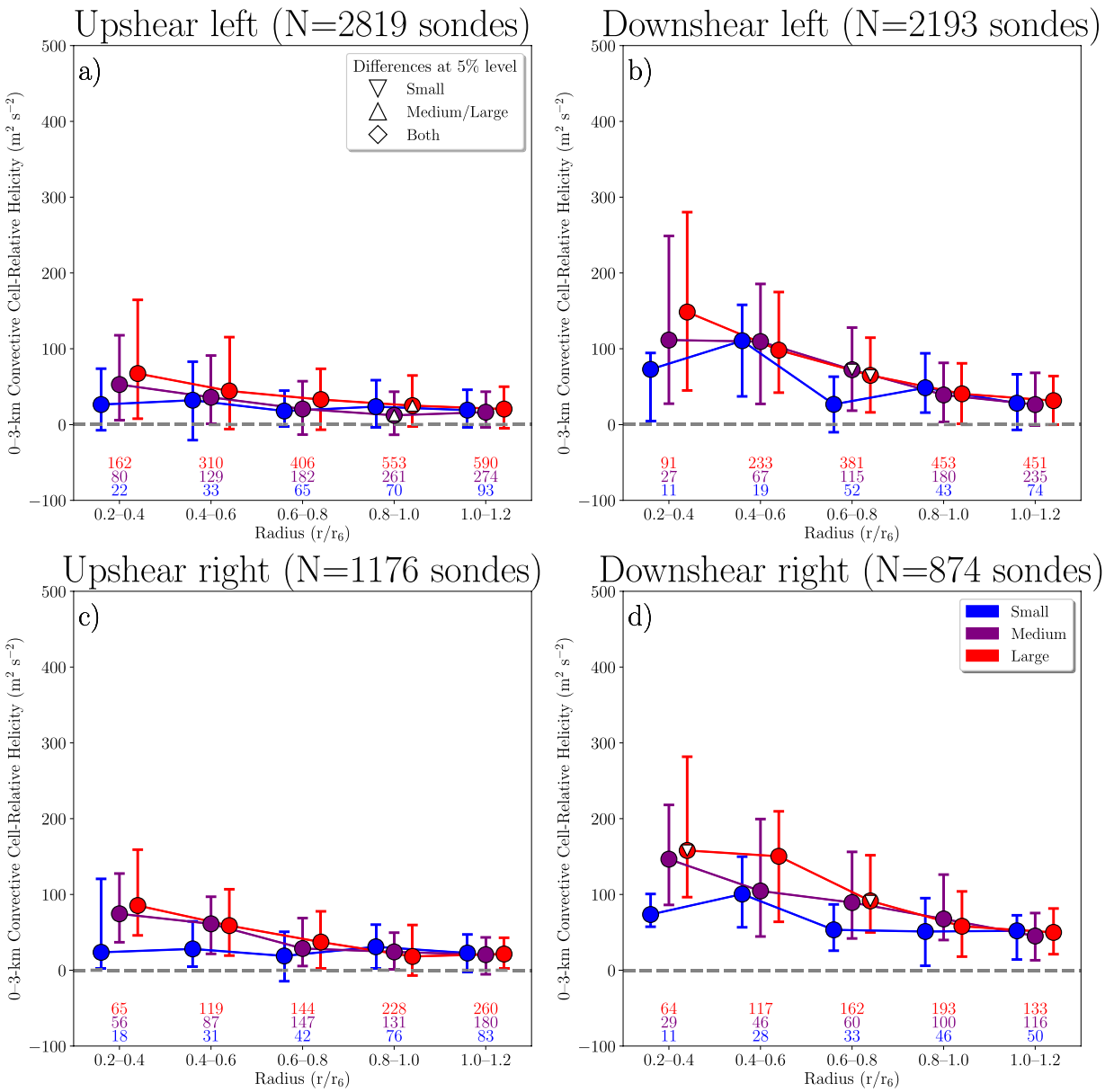

Figure 4. Radial plot of the median (solid line with dots) and the interquartile range (bars) of 0–3-km convective cell-relative helicity (m^2 s^{-2}) for small, medium, and large tropical cyclones (TCs) in the (a) upshear left, (b) downshear left, (c) upshear right, and (d) downshear right quadrants for a radial coordinate normalized by TC outer size (r/r$_6$).

of 6-h large TC times) compared to small TCs (11% of 6-h times) and greater total numbers given that landfalling TCs are most often large. Moreover, larger TCs are also most frequently associated with higher levels of tornadoes per 6 h (i.e., ≥5). However, these enhanced numbers of tornadoes are not due to the increased numbers per unit area as shown by the absence of systematic differences in Figure 3b. Instead, these results suggest a broader region with favorable environments for tornadoes in larger TCs. (Hill et al., 1966; McCaul, 1991).

3.3. Convective-Scale Environments

Larger TCs are associated with broader regions of favorable kinematic environments for tornadoes (Figure 4). Specifically, there are no systematic significant differences in helicity in any quadrant for larger TCs in a radial coordinate normalized by outer size. Median values generally exceed those associated with TC tornadoes (i.e.,

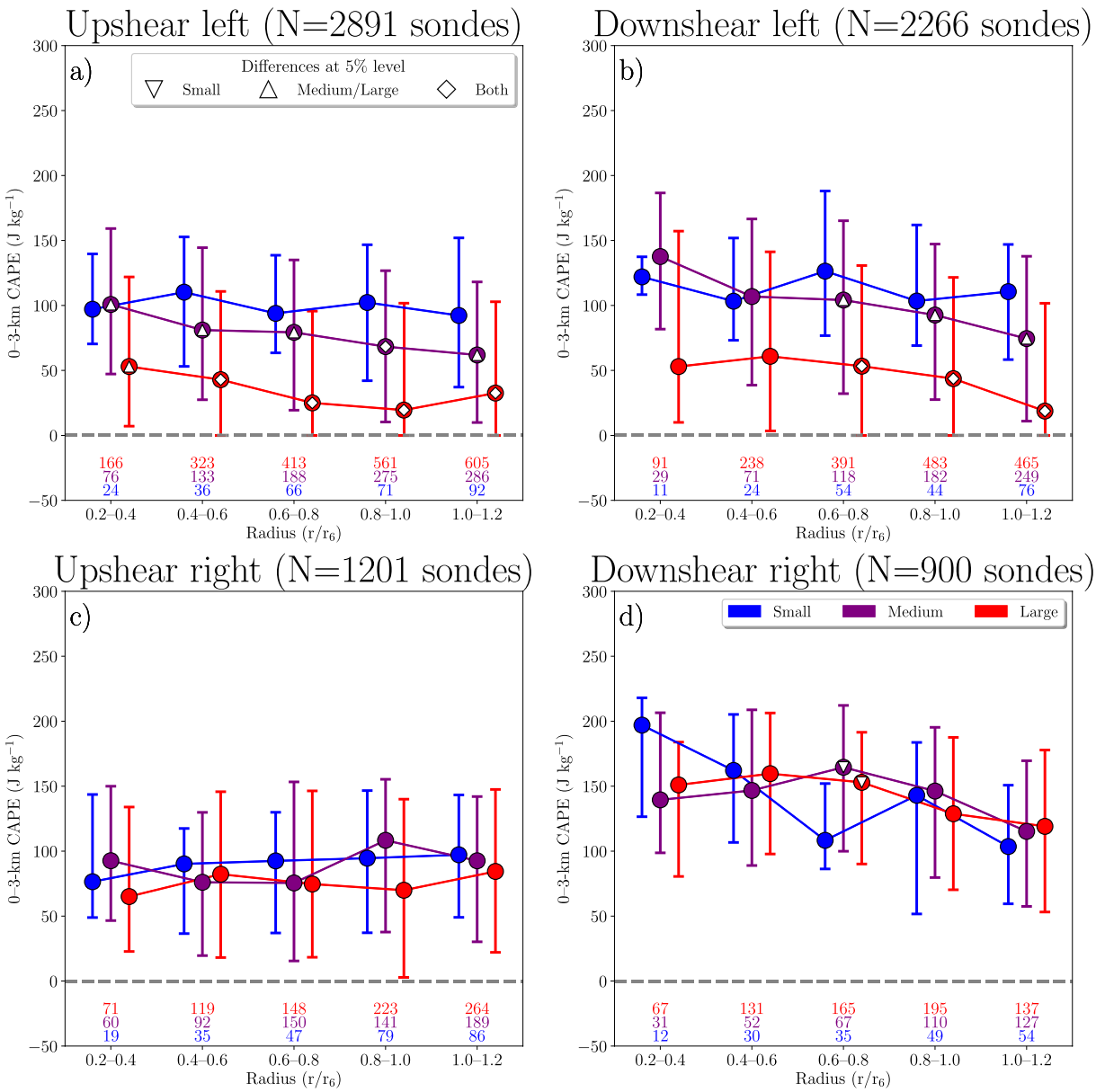

Figure 5. As in Figure 4, but for 0–3-km CAPE(J kg^{-1}).

≥100 m^2 s^{-2}; McCaul & Weisman, 1996; McCaul et al., 2004) over the same subset of normalized radii for both downshear quadrants among outer size bins (i.e., ≤0.4r_6 downshear left, ≤0.6r_6 downshear right; McCaul, 1991). The downshear right quadrant shows slightly larger, yet nonsignificant, differences between helicity in large TCs and the remaining subsets. However, Figure S2 shows systematic increases in TC intensity, but not VWS, associated with larger r_6. To reduce conflation with the impact of TC intensity, we reconstruct radial profiles of helicity (Figure S3) using only those TCs in the lowest intensity tercile computed from the NHC Best Track (Figure S4). Figure S5 shows that these radial profiles of helicity still qualitatively match Figure 4. A similar analysis of the relationship between Best-Track TC intensity and helicity using only large TCs shows no relationship especially at outer radii (Figures S5–S8).

Analysis of convective-scale thermodynamic environments show reduced 0–3-km CAPE in the left-of-VWS-vector quadrants in large TCs compared to small and medium TCs (Figure 5). Specifically, CAPE is 30–50% smaller in the left-of-shear half of large TCs and below guidelines associated with TC tornadoes (i.e., ≥100 J kg^{-1}; Baker

et al., 2009; Eastin & Link, 2009), potentially due to large TCs occurring at poleward latitudes in more baroclinic environments (Merrill, 1984; Schenkel et al., 2018). In contrast, CAPE in the right-of-shear half of the TC shows no sensitivity to outer size. Similar plots stratified by TC intensity, rather than outer size, also show no systematic differences among intensity groupings (Figure S6). Together, these results suggest that larger TCs are associated with an expansion in the radii with favorable helicity downshear, where nearly all tornadoes are found, while CAPE reductions in the left-of-shear quadrants suggest decreases in tornado occurrence. These CAPE decreases may partially offset increases in radii with favorable helicity limiting additional increases in both the area and number of tornadoes with larger TC outer sizes.

4. Summary

This study examined the relationship between the outer size of the TC wind field with tornado occurrence and their associated convective-scale environments. Our analysis showed that TCs with larger outer sizes typically spawn tornadoes farther from the center over a broader region, although these changes do not completely scale with outer size. Larger TCs also more frequently spawn ≥1 tornado per 6 h, especially enhanced numbers of tornadoes (i.e., ≥5) compared to small TCs. Normalization of the number of tornadoes per 6 h by the TC downshear sector shows similar values among outer size categories. This result suggests that larger TCs produce more tornadoes due to a broader region of favorable environments rather than more efficent tornado occurrence per unit area.

These differences in tornado location and frequency with outer size were attributed to a growth in the area of favorable 0–3-km convective-cell relative helicity in the downshear half of larger TCs. These changes approximately scale with outer size yielding a broader region of favorable environments. Helicity was also shown to be more sensitive to TC outer size than intensity. CAPE, however, decreases in the left-of-shear half of large TCs below thresholds associated with tornadoes, which may partially offset the increased area of favorable tornadic environments due to greater helicity.

Together, these results show that TC outer size strongly impacts both tornado frequency and distance, likely due to broader regions of kinematically favorable environments for tornadoes. This study addresses fundamental questions about the relationship between TC outer size and tornadoes left unresolved by prior work (Hill et al., 1966; McCaul, 1991). Finally, these results may shed light on how the location and scale of the TC rain bands change with outer size.

Data Availability Statement

SPC TCTOR are available at https://doi.org/10.5281/zenodo.5719433. Best-Track TC data are available from the NHC (https://www.ncdc.noaa.gov/ibtracs/index.php?name=ib-v4-access), and ERA-5 data was obtained from the NCAR RDA (https://rda.ucar.edu/datasets/ds633.0/). All plots were made in Matplotlib (Hunter, 2007). Severe-weather metrics were calculated using SHARPpy (Blumberg et al., 2017).

Acknowledgments
This work is supported by NSF AGS-1560419 as part of the 2019 National Weather Center REU. Ben Schenkel is supported by NSF AGS-2028151 and funding from OU. This work was completed using the Unidata Science Gateway (https://doi.org/10.5065/688s-2w73) supported by NSF-1901712. The authors would like to thank two anonymous reviewers, Suzana Camargo (Columbia), Daphne LaDue (CAPS/OU), Tom Galarneau (NSSL), Ping Zhu (FIU), and John Knaff (CIRA) for constructive conversations.

References

Alford, A. A., Zhang, J. A., Biggerstaff, M. I., Dodge, P., Marks, F. D., & Bodine, D. J. (2020). Transition of the hurricane boundary layer during the landfall of Hurricane Irene (2011). *Journal of the Atmospheric Sciences*, *77*, 3509–3531. https://doi.org/10.1175/jas-d-19-0290.1

Baker, A. K., Parker, M. D., & Eastin, M. D. (2009). Environmental ingredients for supercells and tornadoes within Hurricane Ivan. *Weather and Forecasting*, *24*, 223–244. https://doi.org/10.1175/2008waf2222146.1

Bian, G.-F., Nie, G.-Z., & Qiu, X. (2021). How well is outer tropical cyclone size represented in the ERA5 reanalysis dataset? *Atmospheric Research*, *249*, 105339. https://doi.org/10.1016/j.atmosres.2020.105339

Blumberg, W. G., Halbert, K. T., Supinie, T. A., Marsh, P. T., Thompson, R. L., & Hart, J. A. (2017). SHARPpy: An open-source sounding analysis toolkit for the atmospheric sciences. *Bulletin of the American Meteorological Society*, *98*, 1625–1636. https://doi.org/10.1175/BAMS-D-15-00309.1

Brammer, A. (2017). *Tropical cyclone vortex tracker*. (Available online at: https://doi.org/10.5281/zenodo.266194

Bunkers, M., Barber, D., Thompson, R., Edwards, R., & Garner, J. (2014). Choosing a universal mean wind for supercell motion prediction. *Journal of Operational Meteorology*, *2*(11), 115–129. https://doi.org/10.15191/nwajom.2014.0211

Carrasco, C. A., Landsea, C. W., & Lin, Y.-L. (2014). The influence of tropical cyclone size on its intensification. *Weather and Forecasting*, *29*(3), 582–590. https://doi.org/10.1175/waf-d-13-00092.1

Chan, K. T. F., & Chan, J. C. L. (2013). Angular momentum transports and synoptic flow patterns associated with tropical cyclone size change. *Monthly Weather Review*, *141*(11), 3985–4007. https://doi.org/10.1175/mwr-d-12-00204.1

Chavas, D. R., & Emanuel, K. (2010). A QuikSCAT climatology of tropical cyclone size. *Geophysical Research Letters*, *37*, L18816. https://doi.org/10.1029/2010gl044558

Chavas, D. R., Lin, N., & Emanuel, K. (2015). A Model for the complete radial structure of the tropical cyclone wind field. Part I: Comparison with observed structure. *Journal of the Atmospheric Sciences*, *72*(9), 3647–3662. https://doi.org/10.1175/jas-d-15-0014.1

Chavas, D. R., Reed, K. A., & Knaff, J. A. (2017). Physical understanding of the tropical cyclone wind-pressure relationship. *Nature communications*, *8*, 1360. https://doi.org/10.1038/s41467-017-01546-9

Chavas, D. R., & Vigh, J. (2014). QSCAT-R: The QuikSCAT tropical cyclone radial structure dataset. *NCAR Tech*. Note, Volume TN-5131STR, 22 pp. (Available from https://verif.rap.ucar.edu/tcdata/quikscat/dataset/index.php

Chen, J., & Chavas, D. R. (2020). The transient responses of an axisymmetric tropical cyclone to instantaneous surface roughening and drying. *Journal of the Atmospheric Sciences*, *77*, 2807–2834. https://doi.org/10.1175/jas-d-19-0320.1

Davis, C., Snyder, C., & Didlake, A. C. (2008). A vortex-based perspective of eastern Pacific tropical cyclone formation. *Monthly Weather Review*, *136*, 2461–2477. https://doi.org/10.1175/2007mwr2317.1

Demuth, J., DeMaria, M., & Knaff, J. (2006). Improvement of advanced microwave sounding unit tropical cyclone intensity and size estimation algorithms. *Journal of applied meteorology and climatology*, *45*, 1573–1581. https://doi.org/10.1175/jam2429.1

Durre, I., Vose, R. S., & Wuertz, D. B. (2006). Overview of the integrated global radiosonde archive. *Journal of Climate*, *19*, 53–68. https://doi.org/10.1175/jcli3594.1

Eastin, M. D., & Link, M. C. (2009). Miniature supercells in an offshore outer rainband of Hurricane Ivan (2004). *Monthly Weather Review*, *137*, 2081–2104. https://doi.org/10.1175/2009mwr2753.1

Edwards, R. (2010), Tropical cyclone tornado records for the modernized National Weather Service era. In *Proceedings 25th conference on severe local storms* (p. P3.1). Denver, CO.

Edwards, R. (2012). Tropical cyclone tornadoes: A review of knowledge in research and prediction. *Electron. Journal of Severe Storms Meteorology*, *7*, 1–61.

Edwards, R., Dean, A. R., Thompson, R. L., & Smith, B. T. (2012). Convective modes for significant severe thunderstorms in the contiguous United States. Part III: Tropical cyclone tornadoes. *Weather and Forecasting*, *27*, 1507–1519. https://doi.org/10.1175/waf-d-11-00117.1

Emanuel, K. (2004). Tropical cyclone energetics and structure. In E. Federovich, R. Rotunno, & B. Stevens (Eds.), *Atmospheric turbulence and mesoscale meteorology* (pp. 51–71). Cambridge University Press. https://doi.org/10.1017/cbo9780511735035.010

Frank, W. M., & Ritchie, E. A. (1999). Effects of environmental flow upon tropical cyclone structure. *Monthly Weather Review*, *127*, 2044–2061. https://doi.org/10.1175/1520-0493(1999)127<2044:eoefut>2.0.co;2

Franklin, J., Black, M., & Valde, K. (2003). GPS dropwindsonde wind profiles in hurricanes and their operational implications. *Weather and Forecasting*, *18*, 32–44. https://doi.org/10.1175/1520-0434(2003)018<0032:gdwpih>2.0.co;2

Galarneau, T. J., & Davis, C. A. (2013). Diagnosing forecast errors in tropical cyclone motion. *Monthly Weather Review*, *141*, 405–430. https://doi.org/10.1175/mwr-d-12-00071.1

Gentry, R. C. (1983). Genesis of tornadoes associated with hurricanes. *Monthly Weather Review*, *111*, 1793–1805. https://doi.org/10.1175/1520-0493(1983)111<1793:gotawh>2.0.co;2

Gu, J.-F., Tan, Z.-M., & Qiu, X. (2018). The evolution of vortex tilt and vertical motion of tropical cyclones in directional shear flows. *Journal of the Atmospheric Sciences*, *75*(10), 3565–3578. https://doi.org/10.1175/jas-d-18-0024.1

Hersbach, H., Bell, B., Berrisford, P., Hirahara, S., Horányi, A., Muñoz-Sabater, J., Nicolas, J., (2020). The ERA5 global reanalysis. *Quarterly Journal of the Royal Meteorological Society*, *146*, 1999–2049. https://doi.org/10.1002/qj.3803

Hill, E. L., Malkin, W., & Schulz, W. A. (1966). Tornadoes associated with cyclones of tropical origin-Practical features. *Journal of Applied Meteorology and Climatology*, *5*(6), 745–763. https://doi.org/10.1175/1520-0450(1966)005<0745:tawcot>2.0.co;2

Hlywiak, J., & Nolan, D. S. (2021). The response of the near-surface tropical cyclone wind field to inland surface roughness length and soil moisture content during and after landfall. *Journal of the Atmospheric Sciences*, *78*, 983–1000. https://doi.org/10.1175/jas-d-20-0211.1

Hunter, J. D. (2007). Matplotlib: A 2D graphics environment. *Computing in science & engineering*, *9*, 90–95. Retrieved from https://doi.ieeecomputersociety.org/10.1109/MCSE.2007.55. https://doi.org/10.1109/mcse.2007.55

Jones, S. (1995). The evolution of vortices in vertical shear. Part I: Initially barotropic vortices. *Quarterly Journal of the Royal Meteorological Society*, *121*, 821–851. https://doi.org/10.1002/qj.49712152406

Kimball, S., & Mulekar, M. (2004). A 15-Year climatology of North Atlantic tropical cyclones. Part I: Size parameters. *Journal of Climate*, *17*, 3555–3575. https://doi.org/10.1175/1520-0442(2004)017<3555:aycona>2.0.co;2

Knaff, J. A., Longmore, S. P., & Molenar, D. A. (2014). An objective satellite-based tropical cyclone size climatology. *Journal of Climate*, *27*, 455–476. https://doi.org/10.1175/jcli-d-13-00096.1

Landsea, C. W., & Franklin, J. L. (2013). Atlantic hurricane database uncertainty and presentation of a new database format. *Monthly Weather Review*, *141*, 3576–3592. https://doi.org/10.1175/mwr-d-12-00254.1

Lin, N., Lane, P., Emanuel, K. A., Sullivan, R. M., & Donnelly, J. P. (2014). Heightened hurricane surge risk in northwest Florida revealed from climatological-hydrodynamic modeling and paleorecord reconstruction. *Journal of Geophysical Research: Atmospheres*, *119*, 8606–8623. https://doi.org/10.1002/2014jd021584

Martinez, J., Nam, C. C., & Bell, M. M. (2020). On the contributions of incipient vortex circulation and environmental moisture to tropical cyclone expansion. *Journal of Geophysical Research: Atmospheres*, *125*, e2020JD033324. https://doi.org/10.1029/2020jd033324

McCaul, E. W. (1991). Buoyancy and shear characteristics of hurricane-tornado environments. *Monthly Weather Review*, *119*, 1954–1978. https://doi.org/10.1175/1520-0493(1991)119<1954:bascoh>2.0.co;2

McCaul, E. W., Buechler, D. E., Goodman, S. J., & Cammarata, M. (2004). Doppler radar and lightning network observations of a severe outbreak of tropical cyclone tornadoes. *Monthly Weather Review*, *132*, 1747–1763. https://doi.org/10.1175/1520-0493(2004)132<1747:dralno>2.0.co;2

McCaul, E. W., & Weisman, M. L. (1996). Simulations of shallow supercell storms in landfalling hurricane environments. *Monthly Weather Review*, *124*, 408–429. https://doi.org/10.1175/1520-0493(1996)124<0408:sosssi>2.0.co;2

Merrill, R. (1984). A comparison of large and small tropical cyclones. *Monthly Weather Review*, *112*, 1408–1418. https://doi.org/10.1175/1520-0493(1984)112<1408:acolas>2.0.co;2

Molinari, J., Romps, D. M., Vollaro, D., & Nguyen, L. (2012). CAPE in tropical cyclones. *Journal of the Atmospheric Sciences*, *69*, 2452–2463. https://doi.org/10.1175/jas-d-11-0254.1

Molinari, J., & Vollaro, D. (2008). Extreme helicity and intense convective towers in Hurricane Bonnie. *Monthly Weather Review*, *136*, 4355–4372. https://doi.org/10.1175/2008mwr2423.1

Molinari, J., & Vollaro, D. (2010). Distribution of helicity, CAPE, and shear in tropical cyclones. *J. Atmos. Sci.*, *67*, 274–284. https://doi.org/10.1175/2009jas3090.1

Novlan, D. J., & Gray, W. M. (1974). Hurricane-spawned tornadoes. *Monthly Weather Review*, *102*, 476–488. https://doi.org/10.1175/1520-0493(1974)102<0476:hst>2.0.co;2

Rhodes, C. L., & Senkbeil, J. C. (2014). Factors contributing to tornadogenesis in landfalling Gulf of Mexico tropical cyclones. *Meteorological Applications*, *21*, 940–947. https://doi.org/10.1002/met.1437

Rios-Berrios, R., & Torn, R. D. (2017). Climatological analysis of tropical cyclone intensity changes under moderate vertical wind shear. *Monthly Weather Review*, *145*, 1717–1738. https://doi.org/10.1175/mwr-d-16-0350.1

Schenkel, B. A., Coniglio, M., & Edwards, R. (2021). How does the relationship between ambient deep-tropospheric vertical wind shear and tropical cyclone tornadoes change between coastal and inland environments? *Weather and Forecasting*, *36*, 539–566. https://doi.org/10.1175/waf-d-20-0127.1

Schenkel, B. A., Edwards, R., & Coniglio, M. (2020). A climatological analysis of ambient deep-tropospheric vertical wind shear impacts upon tornadoes in tropical cyclones. *Weather and Forecasting*, *35*(5), 2033–2059. https://doi.org/10.1175/waf-d-19-0220.1

Schenkel, B. A., & Hart, R. (2012). An examination of tropical cyclone position, intensity, and intensity life cycle within atmospheric reanalysis datasets. *Journal of Climate*, *25*, 3453–3475. https://doi.org/10.1175/2011jcli4208.1

Schenkel, B. A., Lin, N., Chavas, D., Oppenheimer, M., & Brammer, A. (2017). Evaluating outer tropical cyclone size in reanalysis datasets using QuikSCAT data. *Journal of Climate*, *30*, 8745–8762. https://doi.org/10.1175/jcli-d-17-0122.1

Schenkel, B. A., Lin, N., Chavas, D., Vecchi, G. A., Oppenheimer, M., & Brammer, A. (2018). Lifetime evolution of outer tropical cyclone size and structure as diagnosed from reanalysis and climate model data. *Journal of Climate*, *31*(19), 7985–8004. https://doi.org/10.1175/jcli-d-17-0630.1

Schultz, L. A., & Cecil, D. J. (2009). Tropical cyclone tornadoes, 1950–2007. *Monthly Weather Review*, *137*, 3471–3484. https://doi.org/10.1175/2009mwr2896.1

Spratt, S. M., Sharp, D. W., Welsh, P., Sandrik, A., Alsheimer, F., & Paxton, C. (1997). A WSR-88D assessment of tropical cyclone outer rainband tornadoes. *Weather and Forecasting*, *12*, 479–501. https://doi.org/10.1175/1520-0434(1997)012<0479:awaotc>2.0.co;2

Stovern, D. R., & Ritchie, E. A. (2016). Simulated sensitivity of tropical cyclone size and structure to the atmospheric temperature profile. *Journal of the Atmospheric Sciences*, *73*, 4553–4571. https://doi.org/10.1175/jas-d-15-0186.1

Torn, R. D., & Snyder, C. (2012). Uncertainty of tropical cyclone best-track information. *Weather and Forecasting*, *27*, 715–729. https://doi.org/10.1175/waf-d-11-00085.1

Weatherford, C., & Gray, W. (1988). Typhoon structure as revealed by aircraft reconnaissance. Part I: Data analysis and climatology. *Monthly Weather Review*, *116*, 1032–1043. https://doi.org/10.1175/1520-0493(1988)116<1032:tsarba>2.0.co;2